

## Simulation of silicon clusters and surfaces via tight-binding molecular dynamics

F. S. Khan

*Department of Electrical Engineering, The Ohio State University, Columbus, Ohio 43210  
and Department of Physics, Brookhaven National Laboratory, Upton, New York 11973-6000*

J. Q. Broughton\*

*Condensed Matter Physics Branch, Condensed Matter and Radiation Division,  
Naval Research Laboratory, Washington, D.C. 20375-5000*

(Received 21 September 1988)

A prescription is developed which incorporates the tight-binding total energy for silicon into the molecular-dynamics scheme of dynamical simulated annealing first proposed by Car and Parrinello [Phys. Rev. Lett. **55**, 2471 (1985)]. The total-energy expression of Tománek and Schlüter [Phys. Rev. Lett. **56**, 1055 (1986); Phys. Rev. B **36**, 1208 (1987)] with appropriate cutoff functions to permit molecular-dynamics simulations is used to calculate the forces on the ions and the electronic degrees of freedom. A self-contained description of the total energy expression and the simulation method is presented. The scheme permits efficient quenching to zero-temperature and finite-temperature simulations of silicon clusters and surfaces. This method can perform realistic simulations on large systems of the order of hundreds of atoms with time requirements of the order of tens of Cray XMP/24 central-processing-unit hours. The prescription is tested and benchmarked on ground-state geometries of the  $\text{Si}_3$  cluster and the reconstruction of the  $\text{Si}(100)$  surface.

### I. INTRODUCTION

The heart of a molecular-dynamics simulation is the potential from which the forces on the atoms or molecules are calculated. Traditionally, simple two-body potentials such as the Lennard-Jones potential have been used to perform molecular-dynamics simulations. Unfortunately it is not possible to get a stable silicon diamond structure from a two-body potential with a single minimum. As an improvement, computer simulations have been performed on silicon using sums of two-body and three-body potentials.<sup>1-3</sup> Recently, Stillinger and Weber<sup>3</sup> have proposed a three-body potential for solid and liquid silicon which has been constructed to give a stable bulk silicon diamond structure and to produce reasonable agreement with the experimental liquid structure. This model potential was designed to study the solid-liquid transition in bulk silicon, where the local atomic structure is always very close to being tetrahedral and is not suitable for structures with geometries far from tetrahedral symmetry such as clusters and surfaces.<sup>4</sup> As an example, when applied to the  $\text{Si}_3$  cluster it predicts a ground-state geometry with a  $60^\circ$  bond angle and a metastable state with a tetrahedral angle, in contradiction with more accurate theoretical treatments,<sup>5,6</sup> which predict an angle of around  $80^\circ$ .

In a quantum-mechanical treatment using the Born-Oppenheimer approximation, the ground-state energy of a system of silicon atoms depends on the positions of the ions and the quantum states of the electrons and cannot be simply broken into two-body and three-body pieces for any general configuration of the ions. Recently Car and Parrinello<sup>7</sup> have introduced an efficient method to perform molecular dynamics where the forces on the ions

are calculated directly from the total energy of the ionic and electronic system without needing a parametrized few-body interatomic potential. For the electronic contribution to the total energy, the method actually solves the Schrödinger equation via the local-density-functional approximation with a plane-wave basis set. However, a full-fledged local-density approach increases the computational burden so much that simulations of the order of a few hundred atoms are not possible at present using state-of-the-art supercomputers.

In this paper we follow Car and Parrinello's<sup>7</sup> scheme, but instead of the local-density-functional approach we use a parametrized tight-binding total-energy expression for silicon. We use the total-energy expression due to Tománek and Schlüter<sup>8</sup> which we have modified appropriately by smooth cutoff functions to permit molecular-dynamics simulations. This expression permits large deviations of the atoms from bulk equilibrium bond lengths and contains a Hubbard-like term for charging effects. This energy expression and the similar total energy used by Alerhand and Mele,<sup>9</sup> which also contains the Hubbard term, are both derived from the original parametrization scheme of Chadi.<sup>10</sup> This tight-binding Hamiltonian is much simpler and computationally faster to solve than the more accurate density-functional approximation, and for the structural properties we are interested in, has been shown to give results almost as good as the density-functional approach for silicon clusters.<sup>8</sup> As a comparison of time scales involved, we estimate that our code with tight binding runs about a factor of 20 faster than the corresponding density-functional version. We feel that this scheme is a satisfactory compromise between computational speed and accuracy for present-day simulations of semiconductors. We

show that zero- and finite-temperature simulations for several hundred silicon atoms can be performed in times of the order of tens of Cray XMP/24 central-processing-unit (CPU) hours.

In this paper we give a detailed description of the method of incorporating semiempirical tight binding into the scheme of molecular dynamics, including all the relevant parameters and results of the benchmark tests. It should be pointed out that the method is suitable for both zero-temperature and finite-temperature simulations of bulk silicon as well as clusters and surfaces. We apply the method to ground-state structural properties of the  $\text{Si}_3$  cluster and the  $\text{Si}(100)$  surface to demonstrate the feasibility and accuracy of the method and to obtain benchmark results. The material in this paper is arranged in the following order: In Sec. II the total-energy expression for silicon clusters is outlined, with technical details left for the Appendix. This total-energy expression is applied to the ground state of the  $\text{Si}_3$  cluster and it is shown that, unlike the Stillinger-Weber<sup>3</sup> potential, which predicts a  $60^\circ$  angle, the bond angle is predicted to be  $82^\circ$ . The shape of the total-energy curve of  $\text{Si}_3$  versus bond angle is also shown to be in good agreement with Raghavachari's<sup>6</sup> results. Section III contains a detailed description of the total-energy expression for the  $\text{Si}(100)$  slab used in our surface simulations. The slab consists of 128 silicon atoms arranged in four layers with 64 "hydrogen" atoms tied to the bottom layer to satisfy the unsaturated bonds. Section IV contains a description of the molecular-dynamics method proposed by Car and Parrinello.<sup>7</sup> Technical details about the choice of the "fictitious" mass of the electrons, algorithms to integrate the equations of motion, and methods to satisfy the orthonormality constraints of the electronic wave functions are outlined. The aspects which give this procedure speed advantage are also pointed out. The results of the zero-temperature simulations of the  $\text{Si}(100)$  slab are given in Sec. V, where various reconstructions of the surface with different arrangements of tilted and asymmetric dimers are treated. The magnitude of the tilting and charging of the atoms in the dimers is similar to the results obtained by Alerhand and Mele<sup>9</sup> and Chadi.<sup>11</sup> Finally, Sec. VI gives the results of our benchmark tests. We find that the average time taken for a single time step of the simulation of 128 silicon atoms with 64 fixed hydrogen atoms is about 4 CPU seconds of a Cray XMP/24. This implies that zero- and finite-temperature simulations of systems involving hundreds of atoms can be performed in time scales of the order of tens of hours on state-of-the-art supercomputers.

## II. TOTAL ENERGY FOR SILICON CLUSTERS

Consider  $N$  silicon atoms with coordinates  $\{\mathbf{R}_l\}$ ,  $l=1,2,\dots,N$ , giving  $3N$  degrees of freedom for the atomic coordinates. There are four valence electrons per atom, making it a  $4N$  electron problem. Therefore there are  $4N$  occupied single-particle states. Our problem is nonmagnetic, and thus of these states are spin up and half are spin down, and the total number of independent states  $\{\Psi_i\}$ ,  $i=1,2,\dots,2N$ , is equal to  $2N$ . In the tight-

binding method the  $2N$  independent wave functions are expanded in terms of a basis  $\{\phi_{l\alpha}\}$  consisting of four orbitals  $s$ ,  $p_x$ ,  $p_y$ , and  $p_z$  located on each of the  $N$  atoms; here,  $l$  runs over the  $N$  atoms and  $\alpha$  runs over the four orbitals  $s$ ,  $p_x$ ,  $p_y$ , and  $p_z$ :

$$\Psi_i(\mathbf{r}) = \sum_{l=1}^N \sum_{\alpha=1}^4 c_{l\alpha}^i \phi_{l\alpha}(\mathbf{r}), \quad i=1,2,\dots,2N. \quad (1)$$

Thus there are a total number of  $2N \times 4N = 8N^2$  electronic coordinates  $\{c_{l\alpha}^i\}$  for an  $N$ -atom problem. These numbers give 32, 72, and 131 072 electronic degrees of freedom for a 2-, 3-, and 128-atom system, respectively. The full problem involves  $3N + 8N^2$  ionic and electronic degrees of freedom.

The total energy of the ionic and electronic system  $E^{\text{tot}}[\{\mathbf{R}_l\}, \{c_{l\alpha}^i\}]$  is a function of the ionic coordinates  $\{\mathbf{R}_l\}$  and the electronic coordinates  $\{c_{l\alpha}^i\}$ . This energy is constructed by using the total-energy expression of Tománek and Schlüter,<sup>8</sup> which we have modified for molecular dynamics by including appropriate cutoff functions. This expression is described in detail in the Appendix. Here we give a brief description of the various terms of the total energy:

$$E^{\text{tot}} = E^{\text{BS}} + E_2 - E_3 + E_4, \quad (2)$$

where

$$E^{\text{BS}} = 2 \sum_i^{2N} \langle \Psi_i | H | \Psi_i \rangle - NE_{\text{Si}}^0, \quad (3)$$

$$E_2 = \sum_{l=2}^N \sum_{l'=1}^{l-1} E_r(|\mathbf{R}_l - \mathbf{R}_{l'}|), \quad (4)$$

$$E_3 = N \left[ \phi_1 \left( \frac{n_b}{N} \right)^2 + \phi_2 \left( \frac{n_b}{N} \right) + \phi_3 \right], \quad (5)$$

and

$$E_4 = U \sum_{l=1}^N (q_l - q_l^0)^2. \quad (6)$$

$E^{\text{BS}}$  is the tight-binding band-structure energy constructed from Chadi's<sup>10</sup> parametrized nearest-neighbor tight-binding scheme. The matrix elements  $\langle \phi_{l'\alpha'} | H | \phi_{l\alpha} \rangle$  for orbitals on different atoms  $l$  and  $l'$  a distance  $R = |\mathbf{R}_l - \mathbf{R}_{l'}|$  apart are assumed to decay with a factor  $f_c(R)R_0^2/R^2$ ;  $R_0 = 2.35 \text{ \AA}$  is the nearest-neighbor distance in diamond-structure silicon, and  $f_c$  is a smooth cutoff function introduced to allow molecular-dynamics simulations:

$$f_c(R) = \frac{1}{2} \left[ 1 - \tanh \left( \frac{R - R_b}{\Delta} \right) \right]. \quad (7)$$

Here,  $R_b$  is the "bond length" and  $\Delta$  is the scale on which the cutoff function decays. Since Chadi's<sup>10</sup> scheme is a nearest-neighbor fitting scheme,  $R_b$  should have a value which lies between the nearest-neighbor ( $R_0$ ) and the second-nearest-neighbor distance ( $1.63R_0$ ) in diamond silicon and  $\Delta$  should be small enough so that  $f_c(R)$  is negligibly small when  $R$  becomes equal to the second-

nearest distance. For molecular dynamics, on the other hand, we want  $\Delta$  to be reasonably large, otherwise a sharp cutoff will introduce large forces. We get good results by choosing  $R_b = 1.4R_0$  and  $\Delta = 0.1 \text{ \AA}$ .  $E_2$  is the repulsive energy needed to neutralize the effect of double counting of the Coulomb interactions in the band-structure term  $E^{\text{BS}}$ , and also contains the contribution from the exchange correlation energies and the ion-ion interaction.  $E_{\text{Si}}^0$  is the energy of an isolated silicon atom given by  $2(E_s + E_p)$ , where  $E_s \equiv \langle \phi_{1s} | H | \phi_{1s} \rangle$  and  $E_p \equiv \langle \phi_{1x,y,z} | H | \phi_{1x,y,z} \rangle$ . The function  $E_r$  appearing in  $E_2$  is

$$E_r(R) = E_{\text{Si}_2}^{\text{tot}}(R) f_c(R) - E_{\text{Si}_2}^{\text{BS}}(R), \quad (8)$$

where  $E_{\text{Si}_2}^{\text{tot}}$  is the total and  $E_{\text{Si}_2}^{\text{BS}}$  is the band-structure energy of diatomic silicon. For  $E_{\text{Si}_2}^{\text{tot}}$  we use the total energy of the diatomic molecule as calculated by Raghavachari;<sup>12</sup> the full expression for this energy is given in the Appendix.  $f_c$  causes this term to acquire a smooth cutoff; notice that the interatomic matrix elements in  $E_{\text{Si}_2}^{\text{BS}}$  also contain this cutoff function. This term permits the atoms to move arbitrarily far from each other and is suitable for molecular-dynamics simulations. In the original scheme introduced by Chadi<sup>10</sup> and in Alerhand and Mele's<sup>9</sup> scheme, the corresponding term in the total energy is a parametrization obtained by an expansion around the equilibrium positions of the ions in a perfect crystal, and large excursions from equilibrium bond lengths are not permitted. The third term  $E_3$  is needed so that the system will not always favor metallic close-packed coordination.  $n_b$  is the number of bonds,

$$n_b = \sum_{l=2}^N \sum_{l'=1}^{l-1} f_c(|\mathbf{R}_l - \mathbf{R}_{l'}|), \quad (9)$$

and the parameters  $\phi_1$ ,  $\phi_2$ , and  $\phi_3$  are chosen to have the values 0.225, 1.945, and  $-1.03 \text{ eV}$ , respectively; these parameters were chosen by Tománek and Schlüter<sup>8</sup> to reproduce the absolute cohesive energies of both diamond and bcc silicon. Note that with this choice, the term  $E_3$  vanishes for diatomic silicon. The last term  $E_4$  prevents the system from having large charge transfer among the atoms and vanishes for neutral systems. Here,

$$q_l = 2 \sum_{i=1}^{2N} \sum_{\alpha=1}^4 (c_{l\alpha}^i)^2, \quad q_l^0 = 4.0. \quad (10)$$

This term is identical to the charging term of Alerhand and Mele.<sup>9</sup>  $U$  is chosen to be around 1 eV. In agreement with Alerhand and Mele,<sup>9</sup> and Tománek and Schlüter,<sup>8</sup> the results of our calculations are not very sensitive to this choice.

Note that the expression for  $E^{\text{tot}}$  is constructed in such a way that for diatomic silicon ( $N=2$  and  $n_b=1$ ) we get the exact total energy by definition, i.e.,  $E^{\text{tot}} = E_{\text{Si}_2}^{\text{tot}}$ . Also note that if one follows the scheme of minimizing  $E^{\text{tot}}$  with respect to the electronic coordinates  $\{c_{l\alpha}^i\}$  via a matrix diagonalization, then the presence of the last term,  $E_4$ , makes the problem nonlinear and thus requires an iterative self-consistent diagonalization.

Tománek and Schlüter<sup>8</sup> have used this total-energy expression to calculate cohesive energies and equilibrium geometries of isolated silicon clusters by performing a global search for the minimum of (2). They treat clusters of up to a size of 14 atoms and compare the results of this tight-binding calculation with the results of a local-density-functional formalism; they find that the results of the tight-binding calculations are surprisingly similar to the local-density-functional results. Tománek and Schlüter's<sup>8</sup> total-energy expression does not contain a cutoff function; instead, the number of bonds and the nearest neighbors for bonding are judged on a case-by-case basis for each cluster. The introduction of  $f_c$  in (2) automates this process and makes this total-energy function suitable for molecular dynamics.

Recently careful calculations of the ground-state energy of the  $\text{Si}_3$  cluster have appeared in the literature;<sup>5,6</sup> therefore, in order to test the total-energy expression (2) further we have calculated the ground-state energy surface of  $\text{Si}_3$  using this expression. The results of our calculations are compared with the results of a fourth-order Hartree-Fock method (including electron correlation effects via the Møller-Plesset perturbation theory) obtained by Raghavachari<sup>6</sup> in Fig. 1. The solid lines are our results, while the dashed line shows Raghavachari's<sup>6</sup> calculation. The three atoms of the cluster lie on the vertices of an isosceles triangle characterized by an angle  $\theta$  and length  $\gamma$  shown in the inset in Fig. 1. For a given value of  $\theta$  and  $\gamma$ ,  $E^{\text{tot}}$  is minimized with respect to the electronic degrees of freedom to obtain the total energy of  $\text{Si}_3$ . Each point on the plots in the figure is obtained by fixing the angle  $\theta$  and varying the bond length  $\gamma$  to obtain the minimum of  $E^{\text{tot}}$ . The effect of changing  $R_b$  and  $\Delta$  in

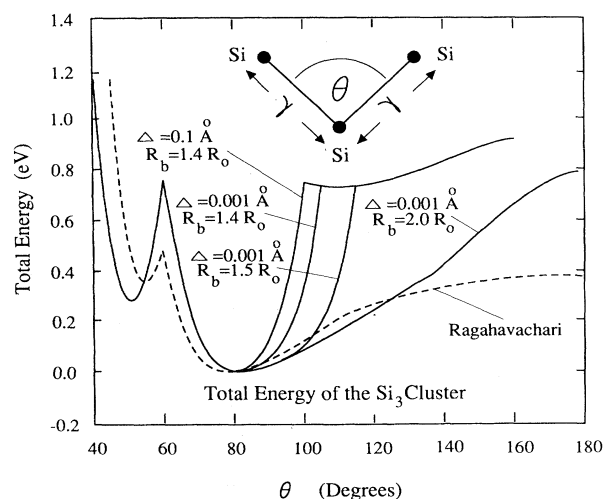


FIG. 1. Ground-state total-energy surface of the  $\text{Si}_3$  cluster obtained by using the total-energy expression (2). The solid lines are our results and the dashed line shows Raghavachari's<sup>6</sup> calculation. The three atoms of the cluster lie at the vertices of an isosceles triangle as shown in the inset. Each point on the solid curves represents the minimum total energy obtained by fixing  $\theta$  and varying  $\gamma$ .  $\Delta$  and  $R_b$  are the width and bond length of the cutoff function (7), respectively.

TABLE I. Ground-state bond length  $\gamma$  and angle  $\theta$  for the  $\text{Si}_3$  cluster (see inset in Fig. 1 for definitions of  $\gamma$  and  $\theta$ ).

	Ground-state $\gamma$ (Å)	Ground-state $\theta$ (deg)
Raghavachari <sup>a</sup>	2.165	77.8
Jones <sup>b</sup>	2.230	85
Present work	2.264	82

<sup>a</sup>Reference 6.

<sup>b</sup>Reference 5.

the cutoff function  $f_c$  are also shown in the figure. Changing  $\Delta$  from 0.1 to 0.001 Å does not cause a big change in the total-energy curve, whereas the effect of changing  $R_b$  from  $1.4R_0$  to  $2.0R_0$  is quite pronounced. The sharp slope discontinuity in our results for  $\theta$  greater than about  $95^\circ$  occurs roughly where the long leg ( $2\gamma \sin\theta/2$ ) of the isosceles triangle exceeds the cutoff distance  $R_b$ , but these tend to occur well away from the ground-state geometry ( $\theta=82^\circ$  and  $\gamma=2.264$  Å). Our calculation with  $R_b=2.0R_0$  shows good agreement with Raghavachari's<sup>6</sup> results. From the figure we see that our results come closer to Raghavachari's<sup>6</sup> over a wider range of angles as  $R_b$  is made larger; however, as mentioned above,  $R_b$  is restricted to remain smaller than the second-nearest-neighbor distance ( $1.63R_0$ ) in diamond silicon because of the nearest-neighbor fitting scheme implicit in the total-energy expression. This suggests that a second-nearest-neighbor fitting scheme (where the restriction on  $R_b$  is less severe) would do a much better job at reproducing the total-energy surfaces of clusters over longer bond lengths. In this light, we are currently working on nonorthogonal full-range tight-binding parametrization schemes. In all the calculations in the rest of this paper we have used a value of  $R_b=1.4R_0$  and  $\Delta=0.1$  Å. The calculations of Jones<sup>5</sup> are based on local-density formalism and are qualitatively similar to the results of Raghavachari.<sup>6</sup> The main features of these calculations along with our results for the  $\text{Si}_3$  cluster are summarized in Table I, which shows that all these calculations are essentially in good agreement among each other. Figure 1 is drawn with the zero of the energy scale set at the minimum of the total-energy curve. In absolute terms using (2) we get  $E^{\text{tot}}=-7.165$  eV at  $\theta=82^\circ$ , which gives a cohesive energy of 2.39 eV per atom, in good agreement with the tight-binding and local-density-functional calculations of Tománek and Schlüter.<sup>8</sup>

### III. TOTAL ENERGY FOR THE Si(100) SLAB

In order to simulate the Si(100) surface we take a slab of four layers of silicon atoms with  $N/4$  atoms per layer. The top layer, in the positive  $z$  direction, forms a surface for which we wish to study possible reconstructions. Periodic boundary conditions are applied in the plane of the surface to simulate a surface extending to infinity in the  $x$  and  $y$  directions. The two unsaturated bonds per atom on the bottom layer, in the negative  $z$  direction, are quenched by tying two hydrogen-like atoms (i.e.  $s$  orbitals) with coordinates  $\mathbf{R}_l^{\text{H}} \pm R_0 \sqrt{2/3} \mathbf{x} - R_0 \sqrt{1/3} \mathbf{z}$  to each

silicon atom  $l$  on the bottom layer, where  $\mathbf{R}_l^{\text{eq}}$  is the equilibrium position of the  $l$ th silicon atom in diamond silicon. Thus the total number of hydrogen atoms  $N_{\text{H}}$  attached to the bottom layer equals  $N/2$ . These "hydrogen" atoms are meant to mimic silicon atoms in the fifth layer and their parameters in the total-energy expression for the slab are chosen to simulate silicon atoms, as explained below.

In our simulations the ionic coordinates of the  $N$  silicon atoms in the top four layers are allowed to take part in the reconstruction, but the ionic coordinates  $\{\mathbf{R}_l^{\text{H}}\}$ ,  $l=1, 2, \dots, N_{\text{H}}$ , of the hydrogen atoms in the fifth layer are kept fixed. Thus the number of ionic degrees of freedom in the problem remain equal to  $3N$ ; on the other hand, the electronic degrees of freedom are increased over the  $N$ -atom silicon problem. Each silicon and hydrogen atom contributes four and one electrons, respectively, giving a total of  $4N+N_{\text{H}}$  electrons. Of the total  $4N+N_{\text{H}}$  occupied single-particle states half are spin up and half are spin down, giving us  $2N+N_{\text{H}}/2$  independent states  $\{\Psi_i\}$ . These states are expanded in terms of a basis set  $\{\phi_{l\alpha}, \phi_l^{\text{H}}\}$  consisting of  $(4N+N_{\text{H}})$  elements, where  $\phi_{l\alpha}$  is a silicon orbital introduced in the preceding section and  $\phi_l^{\text{H}}$  is a "hydrogen"  $s$  orbital located on the hydrogen atom with coordinates  $\mathbf{R}_l^{\text{H}}$ :

$$\Psi_i(\mathbf{r}) = \sum_{l=1}^N \sum_{\alpha=1}^4 c_{l\alpha}^i \phi_{l\alpha}(\mathbf{r}) + \sum_{l=1}^{N_{\text{H}}} c_l^{\text{H}i} \phi_l^{\text{H}}(\mathbf{r}), \quad i=1, 2, \dots, 2N+N_{\text{H}}/2. \quad (11)$$

Thus for our (100) surface problem with  $N/4$  silicon atoms in each of the first four layers and  $N_{\text{H}}=N/2$  hydrogen atom in the fifth layer, the total number of electronic degrees of freedom,  $\{c_{l\alpha}^i, c_l^{\text{H}i}\}$ , is equal to  $(2N+N_{\text{H}}/2) \times (4N+N_{\text{H}}) = 162(N/4)^2$ .

For the total energy  $E^{\text{tot}}$  of this slab, which is a function of the silicon ionic coordinates  $\{\mathbf{R}_l\}$  and the electronic coordinates  $\{c_{l\alpha}^i, c_l^{\text{H}i}\}$ , we modify expression (2) for silicon clusters to include the contribution of the hydrogen atoms:

$$E^{\text{tot}} = E^{\text{BS}} + E_2 - E_3 + E_4, \quad (12)$$

where

$$E^{\text{BS}} = 2 \sum_i^{2N+N_{\text{H}}/2} \langle \Psi_i | H | \Psi_i \rangle - N E_{\text{Si}}^0 - N_{\text{H}} E_{\text{H}}^0, \quad (13)$$

$$E_2 = \sum_{l=2}^N \sum_{l'=1}^{l-1} E_r(|\mathbf{R}_l - \mathbf{R}_{l'}|) + \sum_{l=1}^{N_{\text{H}}} (U_1 X_l + U_2 X_l^2), \quad (14)$$

$$E_3 = N \left[ \phi_1 \left[ \frac{n_b}{N} \right]^2 + \phi_2 \left[ \frac{n_b}{N} \right] + \phi_3 \right], \quad (15)$$

and

$$E_4 = U \sum_{l=1}^N (q_l - q_l^0)^2 + U_{\text{H}} \sum_{l=1}^{N_{\text{H}}} (q_l^{\text{H}} - q_l^{\text{OH}})^2. \quad (16)$$

The various terms in (12) contributed by the silicon atoms have been described in the preceding section; here

we give a brief description of the additional terms due to the hydrogen atoms. For these slab calculations we want the "hydrogen atoms" to behave like silicon atoms; thus, the tight-binding hydrogen-silicon matrix element parameters used in this paper are different from the parameters derived by Allan and Mele,<sup>13</sup> who treat true hydrogen on silicon surfaces. The hydrogen-silicon equilibrium bond length is also different and is set equal to the silicon-silicon bond length. In the band-structure term  $E^{\text{BS}}$  the tight-binding matrix element parameters for the hydrogen-silicon interaction are chosen to be  $E_s^{\text{H}} = -0.117$  eV,  $V_{ss}^{\text{H}} = -2.45$  eV, and  $V_{sp}^{\text{H}} = 3.68$  eV. These parameters were chosen to (a) minimize charge transfer from the bottom silicon layer to the "hydrogens," (b) maintain the Mulliken  $p$ -charge on the fourth-layer silicons at the bulk silicon value, and (c) keep the third- to fourth-layer Mulliken  $ss$  and  $pp$  overlap populations at the bulk nearest-neighbor values. The matrix elements  $\langle \phi_{i\alpha} | H | \phi_j^{\text{H}} \rangle$  decay with a factor  $f_c(R)R_0^2/R^2$ , where  $R = |\mathbf{R}_l - \mathbf{R}_j^{\text{H}}|$  is the interatomic distance, and  $f_c$  is the cutoff function (7). A hydrogen atom is allowed to interact with only the single silicon atom in the fourth layer to which it is attached, and the rest of the silicon-hydrogen matrix elements are set equal to zero; also the interatomic hydrogen-hydrogen matrix elements are assumed to be zero.  $E_{\text{H}}^0 = E_s^{\text{H}}$  is the energy of an isolated hydrogen atom.

Since we do not expect the silicon atoms of the fourth layer to deviate far from the fifth layer of the hydrogen atoms, we follow the scheme proposed by Chadi<sup>10</sup> (in which large excursions from equilibrium bond lengths are not permitted) for the contribution of the hydrogen atoms to the second term  $E_2$  in (12). For  $U_1$  and  $U_2$  we use the values  $-16.31$  and  $49.26$  eV, respectively, were are the values used by Alerhand and Mele<sup>9</sup> for silicon atoms.  $X_l$  is the fractional change in the hydrogen-silicon bond length from its equilibrium bulk value  $R_0$ ,

$$X_l = \frac{|\mathbf{R}_l^{\text{H}} - \mathbf{R}_{l(\text{bottom})}|}{R_0} - 1, \quad (17)$$

for the  $l$ th hydrogen atom which is tied to the single silicon atom  $\mathbf{R}_{l(\text{bottom})}$  in the fourth layer. Because we do not expect the number of hydrogen-silicon bonds to change, there is no contribution to the third term  $E_3$  from the hydrogen layer; the number of bonds  $n_b$  is given by (9). Finally, in the fourth term  $E_4$  we use  $U_{\text{H}} = U$ ; the charges on the silicon and hydrogen atoms  $q_l$  and  $q_l^{\text{H}}$  are given by

$$q_l = 2 \sum_{i=1}^{2N+N_{\text{H}}/2} \sum_{\alpha=1}^4 (c_{l\alpha}^i)^2, \quad q_l^0 = 4.0 \quad (18)$$

and

$$q_l^{\text{H}} = 2 \sum_{i=1}^{2N+N_{\text{H}}/2} (c_i^{\text{Hi}})^2, \quad q_l^{\text{OH}} = 1.0. \quad (19)$$

#### IV. MOLECULAR DYNAMICS FOR THE IONIC AND ELECTRONIC COORDINATES

Now that the total-energy expression has been determined the next step is to simulate the dynamics of the sil-

icon atoms both at zero and at finite temperatures. For ground-state properties we need to minimize the total energy (12) with respect to the ionic and the electronic coordinates. For finite temperatures the electrons can still be kept in their ground state by invoking the Born-Oppenheimer theorem. This means that at all times, for a given instantaneous position of the ions, the total-energy expression should be kept at a minimum with respect to the electronic coordinates, subject to the orthonormality constraints of the wave functions (this minimization is referred to in the literature as quenching the electrons to the Born-Oppenheimer surface). In this paper we use the method proposed by Car and Parrinello<sup>7</sup> to achieve this aim. In this procedure the trajectories of both the ionic and the electronic coordinates are predicted via molecular dynamics, with the forces on the electrons being calculated from a "fictitious Lagrangian."

In order to reduce the number of indices in the mathematics which follows, we combine the coefficients of expansions of the occupied wave function  $i$  [Eq. (11)] into a single vector of dimensionality  $N_T \equiv 4N + N_{\text{H}}$  with elements  $c_m^i$ , whose first  $4N$  elements are defined by  $c_{4(l-1)+\alpha}^i = c_{l\alpha}^i$  and the last  $N_{\text{H}}$  elements are defined by  $c_{4N+l}^i = c_i^{\text{Hi}}$ . In the method of Car and Parrinello<sup>7</sup> these electronic degrees of freedom  $\{c_m^i\}$  are treated as "position" variables of classical particles of fictitious mass  $\mu$ . The dynamics of the silicon ions with mass  $M$  and these fictitious "electrons" is governed by the classical Lagrangian  $L$ ,

$$L = \frac{1}{2}\mu \sum_{i,m} (\dot{c}_m^i)^2 + \frac{1}{2}M \sum_l \dot{\mathbf{R}}_l^2 - E^{\text{tot}}[\{\mathbf{R}_l\}, \{c_m^i\}], \quad (20)$$

and the  $(N_T/2)(N_T/2+1)/2$  number of constraining equations imposed by the orthonormality of the occupied states,

$$\sum_{m=1}^{N_T} c_m^i c_m^j - \delta_{ij} = 0. \quad (21)$$

There are  $3N$  equations of motion for the  $3N$  silicon ionic coordinates,

$$M\ddot{\mathbf{R}}_l = - \frac{\partial E^{\text{tot}}[\{\mathbf{R}_l\}, \{c_m^i\}]}{\partial \mathbf{R}_l}, \quad (22)$$

and for the  $(N_T)^2/2$  electronic coordinates there are an equal number of equations,

$$\mu\ddot{c}_m^i = - \frac{\partial E^{\text{tot}}[\{\mathbf{R}_l\}, \{c_m^i\}]}{\partial c_m^i} + \sum_j \Lambda_{ij} c_m^j. \quad (23)$$

Here,  $i$  and  $j$  run over the occupied states  $1, 2, \dots, N_T/2$ . The matrix  $\Lambda_{ij}$  is a symmetric  $N_T/2 \times N_T/2$  matrix whose elements are the Lagrange multipliers introduced to satisfy the orthonormality constraints of the electronic coordinates given by (21). Since  $\Lambda_{ij}$  is symmetric, there are  $(N_T/2)(N_T/2+1)/2$  independent Lagrange multipliers, and there are an equal number of independent constraining equations (21). The unknowns in this problem are the ionic coordinates  $\{\mathbf{R}_l\}$ , the electronic coordinates  $\{c_m^i\}$ , and the Lagrange multipliers  $\{\Lambda_{ij}\}$ . Note that the number of unknowns is exactly equal to the number of

equations given by (21)–(23) used to determine these unknowns. The Lagrange multipliers are easily determined by differentiating (21) twice with respect to time, giving

$$\Lambda_{ij} = \sum_{m=1}^{N_T} \left[ \frac{1}{2} \frac{\partial E^{\text{tot}}}{\partial c_m^j} c_m^j + \frac{1}{2} c_m^i \frac{\partial E^{\text{tot}}}{\partial c_m^j} - \mu \dot{c}_m^i \dot{c}_m^j \right]. \quad (24)$$

We now outline our method to simulate the dynamics of the ions. For a given position of the ions, the electrons are quenched to the Born-Oppenheimer surface by a self-consistent diagonalization of an  $N_T \times N_T$  Hamiltonian matrix as explained shortly. This accomplishes a minimization of  $E^{\text{tot}}[\{\mathbf{R}_l\}, \{c_{l\alpha}^i\}]$  with respect to the electronic coordinates  $\{c_{l\alpha}^i\}$  for a fixed ionic configuration  $\{\mathbf{R}_l\}$ ; i.e., it corresponds to having the electronic degrees of freedom at the bottom of the potential well  $E^{\text{tot}}[\{\mathbf{R}_l\}, \{c_{l\alpha}^i\}]$  with zero fictitious kinetic energy  $\sum_m \frac{1}{2} \mu (\dot{c}_m^i)^2$ . Now during the molecular-dynamics step, not only are the positions of the ions updated after a time  $\Delta t$  by integrating equation (22) but the “positions” of the electronic coordinates are also updated after this time step by integrating (23) and using (24). For a small enough value of  $\mu$ , the electronic coordinates will remain arbitrarily close to the true Born-Oppenheimer minimum, provided the integrating algorithm is used properly with a small enough  $\Delta t$ . Operationally we set the velocity terms in (24) to zero for reasons given below. This inclusion of the electronic degrees of freedom in the molecular-dynamics step is the important innovation of Car and Parrinello,<sup>7</sup> and we will refer to this as the “fictitious Lagrangian” method. The advantage of this procedure is that for a judicious choice of the fictitious electronic mass  $\mu$  the prediction of the electronic coordinates via Eqs. (23) and (24) keeps the electrons sufficiently close to the Born-Oppenheimer surface for the next  $N_{\text{Born}}$  number of steps, so that the need for a time-costly Born-Oppenheimer quench is obviated during these steps. In our calculations we use  $N_{\text{Born}} = 100$ . Another speed advantage of this scheme is that the “fictitious Lagrangian” method operates only on the coordinates belonging to the occupied subspace of the electronic eigenvectors; the vectors of the unoccupied subspace do not enter.

As mentioned above, to quench the electrons to the Born-Oppenheimer surface we minimize the total energy (12) with respect to the electronic coordinates via self-consistent matrix diagonalization. We employ the Broyden<sup>14</sup> mixing scheme to handle the self-consistent iterations. It can be shown by using the method of Lagrange multipliers that the minimum of  $E^{\text{tot}}$  for a fixed ionic configuration  $\{\mathbf{R}_l\}$  and subject to the constraints (21) is given by

$$E_{\text{min}}^{\text{tot}} = 2 \sum_i^{\text{occ}} \varepsilon_i - N E_{\text{Si}}^0 - N_{\text{H}} E_{\text{H}}^0 + E_2 - E_3 - E_U, \quad (25)$$

where

$$E_U = U \sum_{l=1}^N [q_l^2 - (q_l^0)^2] + U_{\text{H}} \sum_{l=1}^{N_{\text{H}}} [(q_l^{\text{H}})^2 - (q_l^{\text{OH}})^2]. \quad (26)$$

$E_2$  and  $E_3$  have been defined in the preceding section, and  $\sum_i^{\text{occ}} \varepsilon_i$  is the sum of the lowest  $N_T/2$  (occupied) eigenvalues

$\varepsilon_i$  of a self-consistent  $N_T \times N_T$  effective Hamiltonian  $H_{\text{eff}}$  with matrix elements

$$\langle m | H_{\text{eff}} | n \rangle = \langle m | H | n \rangle + 2 U_{(m)} (q_{(m)} - q_{(m)}^0) \delta_{mn}. \quad (27)$$

Here,  $q_{(m)} = q_l$ ,  $q_{(m)}^0 = q_l^0$ ,  $U_{(m)} = U$ , and  $l = I(m/4) + 1$  for  $1 \leq m \leq 4N$ ;  $I(x)$  is defined as the largest integer smaller than  $x$ . For  $4N + 1 \leq m \leq 4N + N_{\text{H}}$  we have  $q_{(m)} = q_l^{\text{H}}$ ,  $q_{(m)}^0 = q_l^{\text{OH}}$ ,  $U_{(m)} = U_{\text{H}}$ , and  $l = m - 4N$ .  $E_U$  corrects for the double counting of the charging term which arises from the sum over the eigenvalues in (25); the charges in  $E_U$  are evaluated by using the  $N_T/2$  eigenvectors of  $H_{\text{eff}}$  corresponding to these occupied eigenvalues.

To update the ionic trajectories  $\mathbf{R}_l(t_n)$  at the  $n$ th molecular-dynamics time step  $t_n = n \Delta T$  we use Beeman's<sup>15</sup> algorithm to integrate the ionic equations of motion (22):

$$\begin{aligned} \mathbf{R}_l(t_{n+1}) &= \mathbf{R}_l(t_n) + \Delta t \dot{\mathbf{R}}_l(t_n) \\ &\quad + \Delta t^2 [4\ddot{\mathbf{R}}(t_n) - \ddot{\mathbf{R}}(t_{n-1})] / 6 + O(\Delta t^4), \end{aligned} \quad (28)$$

$$\begin{aligned} \Delta t \dot{\mathbf{R}}_l(t_{n+1}) &= \mathbf{R}_l(t_{n+1}) - \mathbf{R}_l(t_n) \\ &\quad + \Delta t^2 [2\ddot{\mathbf{R}}(t_{n+1}) + \ddot{\mathbf{R}}(t_n)] / 6 + O(\Delta t^4). \end{aligned} \quad (29)$$

To make the procedure efficient the accelerations should be stored in memory since they are needed more than once in the integration scheme. As far as the memory requirement of this algorithm is concerned, at first sight it appears as if one requires a storage space for  $7 \times 3N$  real numbers; actually the required storage space is  $4 \times 3N$ . To calculate the positions at time  $t_{n+1}$  we need stored positions and velocities at time  $t_n$ . The new positions at  $t_{n+1}$  can be stored in the space used by the velocities at  $t_n$  since the latter are no longer needed. Next, to calculate the velocities at  $t_{n+1}$  we need stored positions at times  $t_n$  and  $t_{n+1}$ . These new velocities can be stored in the space used by the positions at  $t_n$  which are not needed again. Thus, by swapping the storage space for velocities and positions the memory requirement can be made more efficient. A similar situation holds for the accelerations.

The “fictitious Lagrangian” procedure involves updating the trajectories of the electronic coordinates  $c_m^j(t_n)$  along with the ions during  $N_{\text{Born}}$  time steps after each quench to the Born-Oppenheimer surface (when the kinetic energy associated with the electronic degrees of freedom is set equal to zero). The forces (23) on the electronic coordinates at time  $t_n$  depend on the Lagrange multipliers (24). Since the electrons are kept near the Born-Oppenheimer surface during the  $N_{\text{Born}}$  steps, their kinetic energy is always very small and the term in Eq. (24), that depends on the electronic velocities, is always negligibly small; hence, we set this term equal to zero. This simplifies the integration of the equations of motion; otherwise velocities at time  $t_n$  would be needed to calculate positions at time  $t_n$ . Since any algorithm to integrate the equations of motion (23) is approximate, the electronic trajectories will systematically drift away from the constraints (21) as the simulation progresses in time, even

though the forces of constraints are explicitly accounted for in the equations of motion. This results in poor energy conservation. To overcome this problem, we explicitly perform a Gram-Schmidt orthogonalization of the electronic degrees of freedom after each update of the electronic coordinates. Since Gram-Schmidt changes the coordinates from the ones calculated by the integration of the equations of motion, the "electronic" velocities at time  $t_n$  are not appropriate to predict the "electronic" coordinates at time  $t_{n+1}$ . Thus the Beeman<sup>15</sup> algorithm is not suitable and instead we use Verlet's<sup>16</sup> procedure to integrate (23),

$$c_m^i(t_{n+1}) = 2c_m^i(t_n) - c_m^i(t_{n-1}) + \Delta t^2 \ddot{c}_m^i(t_n) + O(\Delta t^4). \quad (30)$$

This coupling of the forces of constraints and the Gram-Schmidt procedure actually produces smooth trajectories. Other orthogonalization schemes such as "shake"<sup>17</sup> or Löwdin<sup>18</sup> are possible. The precise set of vectors obtained via Gram-Schmidt depends upon the order of orthogonalization; we orthogonalize in the order of lowest energy first. This might be expected to put noise into the trajectories of the electronic degrees of freedom. Löwdin and "shake" are expected to give smoother trajectories. For example, the Löwdin scheme finds the set of orthogonal vectors closest in a least-square sense to the input vectors, i.e., those produced by the Verlet step. The Löwdin first-order scheme takes 1.5 times longer than the Gram-Schmidt step. Second-order Löwdin is overkill. Operationally we find identical trajectories whether we use Gram-Schmidt or Löwdin over the 100 time steps ( $N_{\text{Born}} = 100$ ) in between the quenches to the Born-Oppenheimer surface. We also employed the Payne-Joannopoulos<sup>19</sup> scheme instead of (30) in order to determine whether larger time steps could be used. For the tight-binding systems, no advantage was gained over the Verlet integrator.

A few words are in order concerning the fictitious mass  $\mu$  of the "electrons." The value of this mass is entirely arbitrary as long as the electrons are in their ground state with zero kinetic energy. The simulation of the ions is physical only if there is negligible exchange of energy between the ionic and the electronic system and the kinetic energy of the electrons remains approximately zero; i.e., we want the electrons to remain near their ground state at all times and follow the ionic motion adiabatically. In order to ensure adiabatic dynamics, the total energy of the ions,

$$\frac{1}{2}M \sum_I \dot{R}_I^2 + E^{\text{tot}}[\{\mathbf{R}_I\}, \{c_m^i\}], \quad (31)$$

should be a constant of motion for a fixed-energy simulation. Strictly speaking, adiabatic dynamics is obtained only in the limit of an infinitesimally small  $\mu$ . Unfortunately a very small electronic mass requires a small time step  $\Delta t$  with a corresponding increase in the total number of time steps in the simulation. Thus in practice a compromise is reached by choosing  $\mu$  larger enough so that the ionic energy (31) is conserved to within some predetermined tolerance. The values of these parameters

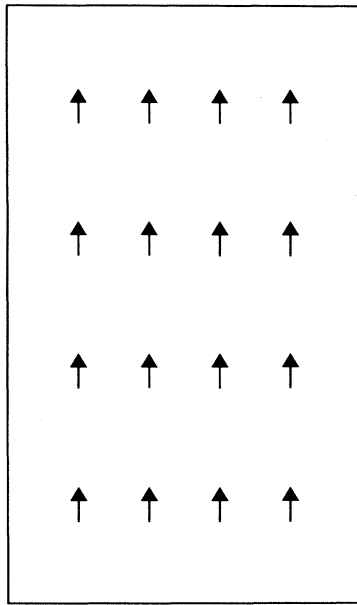
chosen for the simulations in this paper are given in the next section.

It should be pointed out that the method presented in this section can be used for both seeking the zero-temperature ground state and for finite-temperature simulations of the atoms. A number of methods are available for simulating systems at finite temperatures via molecular dynamics<sup>20</sup> which can be readily applied to the scheme outlined here. These methods are based on the fact that for a system of  $N$  classical particles at a temperature  $T$  the canonical average of the total kinetic energy equals  $3Nk_B T/2$ , where  $k_B$  is the Boltzmann constant. In the simplest of these methods most commonly used, the velocities of all the classical ions are scaled periodically to give a total kinetic energy equal to  $3Nk_B T/2$  corresponding to a given fixed temperature  $T$ . Thus energy is either pumped into or extracted from the system to simulate a heat bath at temperature  $T$ . The Beeman<sup>15</sup> algorithm is particularly suitable for velocity rescaling.

## V. RESULTS OF Si(100) SLAB CALCULATIONS

The aim of this paper is to develop a method based on tight-binding molecular dynamics which can be used to study silicon clusters and surfaces, both at zero and at finite temperatures. We now illustrate how our algorithm can be used in a "simulated quenching" mode to find metastable ionic coordinates for a series of candidate ground states for the Si(100) surface. Although the ground state of Si(100) has been studied before by tight binding<sup>9,11</sup> we treat this surface here for the following reasons. (i) To study the feasibility of this method and perform benchmarks to determine its advantages over other methods; the results of these benchmarks are presented in the next section. (ii) To test the accuracy of this method; towards this aim we use Alerhand and Mele's<sup>9</sup> total-energy expression in our method and compare the results with those of Ref. 9. (iii) To obtain the ground-state properties predicted by the total-energy expression (12), which is more suitable for molecular dynamics than the energy expression of Ref. 9.

A truncated  $1 \times 1$  Si(100) surface contains many unsaturated bonds and the system tends to minimize its energy by reconstructing its surface. Theoretical<sup>9,11,21</sup> and experimental<sup>22</sup> evidence shows that this reconstruction causes dimers to appear on the surface; i.e., surface atoms move toward each other to form pairs. Furthermore, these dimers are tilted and asymmetric with respect to terminated bulk. The tilting is accomplished by a charge transfer from one of the atoms of the dimer to the other, which makes it necessary to introduce the charging term  $E_4$  in the total-energy expression (12) and turns the problem into a self-consistent one. To add to the richness of this problem, the dimers can arrange themselves in various patterns on the surface with different supercells and thus many reconstructions of the surface are possible.<sup>9,11,23</sup> In this paper we study a few important reconstructions for the Si(100) surface, namely the  $(2 \times 1)$ ,  $(4 \times 1)$ ,  $c(4 \times 2)$ , and the  $p(2 \times 2)$  reconstructions belonging to the "2x1" family and the  $c(2 \times 2)$  reconstruction belonging to the "c(2x2)" family. The notation of Ref.

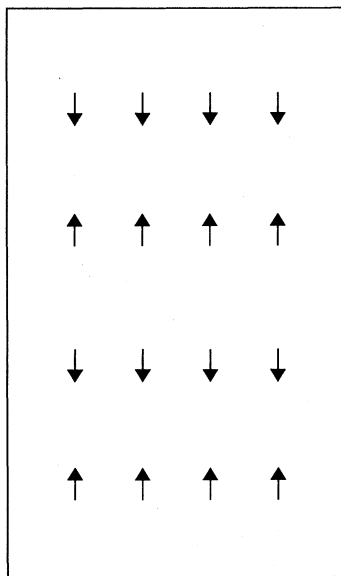


Si (100) (2 x 1)

FIG. 2. Dimers on the surface of the supercell used in our (2×1) Si(100) ("2×1" family) simulations. Each arrow represents a dimer with the tip indicating the up atom.

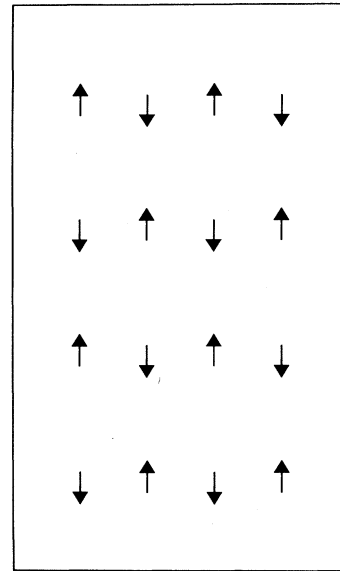
23 has been used to categorize the various reconstructions. The arrangement of the dimers in these reconstructions are shown in Figs. 2–6; each arrow in the figures represents a single dimer with the tip of the arrow indicating the up atom.

Our system consists of 128 silicon atoms and 64 hydro-



Si (100) (4 x 1)

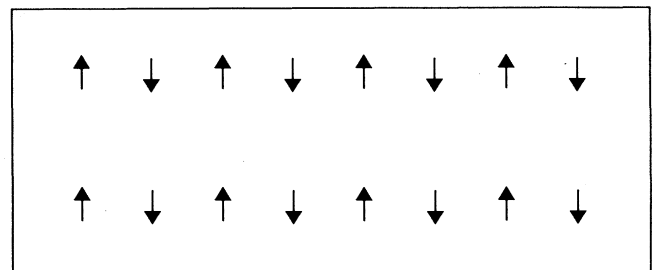
FIG. 3. Dimers on the surface of the supercell used in our (4×1) Si(100) ("2×1" family) simulations. Each arrow represents a dimer with the tip indicating the up atom.



Si (100) C(4 x 2)

FIG. 4. Dimers on the surface of the supercell used in our c(4×2) Si(100) ("2×1" family) simulations. Each arrow represents a dimer with the tip indicating the up atom.

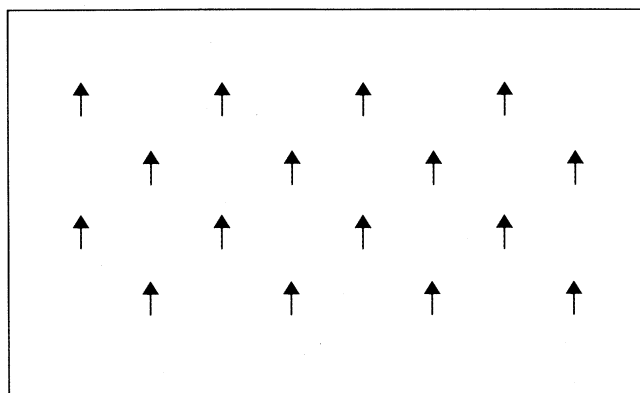
gen atoms. Figures 2–6 qualitatively show the actual number and arrangement of atoms for the surface of the supercell used in our slab calculations. Keeping in mind that periodic boundary conditions are applied in the plane of the surface, these figures can be used to determine the number and position of  $\mathbf{k}$  points in the irreducible Brillouin zone of the primitive lattice of the respective reconstructed surface. With a choice of the fictitious electronic mass  $\mu = (15.04) \times (\text{actual electronic mass})$ ,  $N_{\text{Born}} = 100$  and the molecular-dynamics time step  $\Delta t = 10^{-16}$  s, the total energy of the ions (31) is conserved to within a tolerance of one part in  $10^6$  over the course of at least 3000 updates. The simulation was performed in the following manner. To start a run for a given symmetry, the atoms on the surface were arranged as symmetric



Si (100) P(2 x 2)

FIG. 5. Dimers on the surface of the supercell used in our p(2×2) Si(100) ("2×1" family) simulations. Each arrow represents a dimer with the tip indicating the up atom.





Si (100) C(2 × 2)

FIG. 6. Dimers on the surface of the supercell used in our  $c(2 \times 2)$  Si(100) [ $c(2 \times 2)$  family] simulations. Each arrow represents a dimer with the tip indicating the up atom.

dimers with the given symmetry and an arbitrarily chosen uniform tilting for all the dimers. As the simulated quench proceeded in time the kinetic energy of the ions was periodically and carefully quenched to keep the system from overheating and jumping into another metastable well with a different symmetry. The electrons were quenched to the Born-Oppenheimer surface after every 100 steps, i.e.,  $N_{\text{Born}} = 100$ . A typical run to reach an energy minimum required approximately 4000 molecular-dynamics time steps. We consider the system to be sufficiently close to an energy minimum if its temperature does not increase by more 0.5 K in 400 molecular-dynamics time steps; with this criteria our total energies per atom are reliable to  $\pm 10^{-3}$  meV.

To test our procedure we first use Alerhand and Mele's<sup>9</sup> total-energy expression instead of the total energy (12) and apply it to the Si(100)  $2 \times 1$  reconstruction. A comparison with their results is given in Table II, which shows that the two sets of results are in good agreement. Slight differences are due to the fact that we use the tight-binding matrix-element parameters of Ref. 10 instead of Ref. 9. The surface dimer tilt in this paper is denoted by  $\delta z$  and charge transfer  $\delta q$  between the atoms

TABLE II.  $2 \times 1$  Si(100) reconstruction using Alerhand and Mele's<sup>9</sup> Hamiltonian. Note that since the Hubbard-like on-site charging term as defined in Ref. 9 differs from the corresponding term in our paper by a factor of two;  $2U = 1.9$  eV in this table corresponds to  $U_A = 1.9$  eV as defined by Alerhand and Mele.

	$\delta z$ (Å)	$\delta q$
Alerhand and Mele, <sup>a</sup> $U = 0.0$ eV	0.59	0.39
Present work, $U = 0.0$ eV	0.59	0.39
Alerhand and Mele, <sup>a</sup> $2U = 1.9$ eV	0.58	0.23
Present work, $2U = 2.0$ eV	0.58	0.16

<sup>a</sup>Reference 9.

of the dimer is defined as

$$\delta q = (q_l - q_{l'})/2, \quad (32)$$

where  $q_l$  and  $q_{l'}$  are the charges on the two atoms  $l$  and  $l'$  of the dimer. Finally we use the total-energy expression (12) of Tománek and Schlüter<sup>8</sup> modified for molecular dynamics by the appropriate cutoff functions described in Secs. II and III. These results are summarized in Table III for the case where the on-site charging parameter  $U$  is set equal to 0 and in Table IV for the case  $U = 1.0$  eV. In both cases, the  $p(2 \times 2)$  structure had the lowest energy and is presumed to be the ground state. In these tables,  $\Delta E^s$  for a given reconstruction  $X$  is defined as the relative surface energy per unit surface atom with respect to the  $p(2 \times 2)$  ground state reconstruction  $G$ , i.e.,

$$\Delta E^s = \frac{E^{\text{tot}}(X) - E^{\text{tot}}(G)}{N_S}, \quad (33)$$

where  $N_S$  is the number of surface atoms ( $N_S = 32$  in our calculations). The tables show that the  $c(2 \times 2)$ ,  $c(4 \times 2)$ , and  $p(2 \times 2)$  reconstructions are almost degenerate, both for  $U = 0$  and 1.0 eV. These results are similar to published results of the Si(100) surface using tight binding.<sup>9,11</sup>

## VI. BENCHMARKS AND CONCLUSIONS

The computer code was run on a Cray XMP/24. To increase the performance of the simulation we use the standard techniques of molecular dynamics to optimize speed, such as constructing neighbor (Verlet) lists of atoms which are updated infrequently.<sup>20</sup> Because nearest-neighbor tight binding implies a finite range of interaction between atoms, the use of Verlet lists turns many of the  $(M \times M)$ -order matrix multiplications (e.g., the product of the Hamiltonian and coefficient matrices) from order  $M^3$  to order  $M^2$  processes. As a function of system size  $N_T$ , our programs scale as  $N_T^{2.5}$ . The code is written in FORTRAN and the do loops are constructed with an eye towards easy vectorization. Cray subroutines for finding matrix eigenvalues and eigenvectors are used and most of the code has been written so that it functionally looks like the inner product of large vectors. Cray routines are used for dot products. The speed advantage of vectorizing alone was benchmarked to be around a factor of three.

Our system consisting of 128 silicon atoms and 64 hydrogen atoms needs about 2.6 Cray megawords of memory. The effective Hamiltonian matrix (27) has the dimensionality of  $576 \times 576$ ; one quench to the Born-Oppenheimer surface involves iterated (self-consistent) diagonalization of this matrix. Our benchmarks show that a single time step without quenching to the Born-Oppenheimer surface takes about 3.5 CPU seconds and a full quench to the Born surface takes around 23 s per self-consistent iteration of the matrix diagonalization. We find that typically the self-consistent diagonalization requires only about two iterations, but occasionally it may require five or even as high as ten iterations of this time-costly step; this happens when the energy band gap between the occupied and unoccupied states of the Hamiltonian  $H_{\text{eff}}$ , Eq. (27), becomes very small, i.e., the system

TABLE III. Si(100) reconstructions using the total-energy expression (12) with the Hubbard-like on-site charging parameter  $U=0.0$  eV. For the symmetries and families of reconstructions the nomenclature of Ref. 23 is used.  $N_T$  is the total number of silicon and “hydrogen” atoms in the slab.

Symmetry	Family	$E^{\text{tot}}/N_T$ (eV/atom)	$\Delta E^s$ (meV/surf. atom)	$\delta z$ (Å)	$\delta q$
(2×1)	“2×1”	−4.825 21	180.13	0.66	0.35
(4×1)	“2×1”	−4.833 51	130.32	0.15	0.14
<i>c</i> (2×2)	“ <i>c</i> (2×2)”	−4.851 30	23.59	0.43	0.34
<i>c</i> (4×2)	“2×1”	−4.854 23	5.99	0.47	0.36
<i>p</i> (2×2)	“2×1”	−4.855 23	0.00	0.47	0.36

approaches semimetallic behavior. Recalling that  $N_{\text{Born}}=100$ , this translates into about a 4-s typical time step and a 4.6–5.8-s average time step when the band gap is small. We estimate that the number of time steps required for a realistic simulation at finite temperatures is around 10 000, which translates into 10–16 Cray XMP/24 CPU hours if the algorithm presented in this paper is used.

The benchmark figures mentioned above show that the time advantage gained by using this method over the straightforward molecular-dynamics approach (in which the electrons are quenched to the Born surface at each time step via a self-consistent matrix diagonalization) is typically a factor of 12 and sometimes as high as a factor of 40. As mentioned before, one reason for the efficiency of the “fictitious Lagrangian” scheme is that it operates only upon the coordinates belonging to the occupied electronic states. However, the advantage is smaller for tight binding, where the number of occupied states  $N_{\text{occ}}$  is half the number of elements in the basis set  $N_{\text{basis}}$ , than in methods based on plane waves where  $N_{\text{occ}} \ll N_{\text{basis}}$ . Our algorithm achieves its main speed advantage by performing the most time-costly step of matrix diagonalization infrequently. A potential drawback of this method could be that one is restricted to use a comparatively small time steps  $\Delta t$  of the simulation because the adiabatic dynamics imposed by the “fictitious Lagrangian” method restricts the “electronic” mass  $\mu$  to be small. However, our tests show that for our total-energy expression, even if we quench to the Born-Oppenheimer surface at every time step,  $\Delta t$  cannot be increased by more than a factor of 1.7 over the one we are using in this paper ( $10^{-16}$  s), if good energy conservation is required. By carefully adjusting

the fictitious electronic mass  $\mu$ , the tolerance for energy conservation, and  $N_{\text{Born}}$ , one can increase  $\Delta t$  to  $1.7 \times 10^{-16}$  s even within our scheme; we, however, remain on the conservative side and use  $10^{-16}$  s. Štich<sup>24</sup> has recently developed an energy-minimization scheme based on conjugate gradient methods, which is more efficient than large matrix diagonalization. The expectation was that one could use straightforward molecular dynamics by quenching to the Born surface at each time step and by-pass the “fictitious Lagrangian” procedure. Unfortunately, quenching the electrons to the ground state at each time step yields trajectories for the ions which diverge from the real trajectories because of a systematic addition of small errors generated by the finite precision of the minimization scheme. In the method of molecular dynamics with the “fictitious Lagrangian” step, the electrons respond to Newtonian equations, and, because of inertial overshoot effects, the errors cancel instead of adding systematically. Thus another major advantage of this approach is that the ionic trajectories are more reliable. One might also consider quenching to the Born-Oppenheimer surface by the conjugate gradient procedure instead of the self-consistent diagonalization every  $N_{\text{Born}}$  steps. We have used a steepest-descent algorithm in this manner and found it to be of marginal improvement over diagonalization, the reason being that the Born-Oppenheimer quench occurs sufficiently infrequently that the overall speed of the simulation is not very sensitive to the particular minimization scheme used.

In conclusion, we have successfully incorporated the tight-binding total-energy expression of Tománek and Schlüter<sup>8</sup> into the scheme of molecular dynamics with simulated annealing first proposed by Car and Parrinell-

TABLE IV. Si(100) reconstructions using the total-energy expression (12) with the Hubbard-like on-site charging parameter  $U=1.0$  eV. For the symmetries and families of reconstructions the nomenclature of Ref. 23 is used.  $N_T$  is the total number of silicon and “hydrogen” atoms in the slab.

Symmetry	Family	$E^{\text{tot}}/N_T$ (eV/atom)	$\Delta E^s$ (meV/surf. atom)	$\delta z$ (Å)	$\delta q$
(2×1)	“2×1”	−4.811 73	201.47	0.69	0.17
(4×1)	“2×1”	−4.831 32	83.88	0.11	0.04
<i>c</i> (2×2)	“ <i>c</i> (2×2)”	−4.843 31	11.98	0.42	0.13
<i>c</i> (4×2)	“2×1”	−4.844 50	4.87	0.47	0.15
<i>p</i> (2×2)	“2×1”	−4.845 31	0.00	0.48	0.15

lo.<sup>7</sup> The scheme permits efficient zero-temperature and finite-temperatures simulations of silicon clusters and surfaces. We have demonstrated that this method can handle large systems of the order of hundreds of atoms and the time required for realistic simulations is of the order of tens of Cray XMP/24 CPU hours.

#### ACKNOWLEDGMENTS

We thank P. B. Allen and M. A. Schlüter for helpful discussions. This work was supported in part by the Division of Material Science, Office of Basic Energy Sciences, U.S. Department of Energy under Contract No. DE-AC02-76CH00016. One of us (F.S.K.) also gratefully acknowledges support through a grant from Cray Research, Inc. and the Ohio Supercomputer Center for the allocation of computing resources. The work of J.Q.B. was supported in part by the U.S. Office of Naval Research.

#### APPENDIX: TOTAL ENERGY FOR SILICON CLUSTERS

This Appendix contains a detailed description of Tománek and Schlüter's<sup>8</sup> expression for the parametrized tight-binding total energy of silicon clusters. The expression has been modified to permit molecular-dynamics simulations by introducing appropriate smooth cutoff functions. The total-energy expression (2) has already been introduced in Sec. II of this paper; here we treat the various terms involved in detail.

##### 1. The band structure term $E^{\text{BS}}$

The band structure term, Eq. (3), is

$$E^{\text{BS}} + NE_{\text{Si}}^0 = \sum_i^{\text{occ}} \langle \Psi_i | H | \Psi_i \rangle = 2 \sum_{i=1}^{2N} \langle \Psi_i | H | \Psi_i \rangle$$

$$= 2 \sum_{i=1}^{2N} \sum_{l', \alpha'} \sum_{l, \alpha} c_{l', \alpha'}^i c_{l, \alpha}^i \langle l', \alpha' | H | l, \alpha \rangle, \quad (\text{A1})$$

where  $\langle \phi_{l', \alpha'} | H | \phi_{l, \alpha} \rangle \equiv \langle l', \alpha' | H | l, \alpha \rangle$  and  $E_{\text{Si}}^0$  is the energy of an isolated silicon atom given by  $2(E_s + E_p)$ , where  $E_s \equiv \langle \phi_{1s} | H | \phi_{1s} \rangle$  and  $E_p \equiv \langle \phi_{l, \alpha} | H | \phi_{l, \alpha} \rangle$ . This term can be rewritten as

$$E^{\text{BS}} + NE_{\text{Si}}^0 = 2 \sum_{i=1}^{2N} \sum_{l=1}^N \sum_{\alpha=1}^4 (c_{l, \alpha}^i)^2 \times \begin{cases} E_x & \text{if } \alpha=1 \\ E_p & \text{if } \alpha=2, 3, 4 \end{cases}$$

$$+ 4 \sum_{i=1}^{2N} \sum_{l=2}^N \sum_{l'=1}^{l-1} \sum_{\alpha=1}^4 \sum_{\alpha'=1}^4 c_{l, \alpha}^i c_{l', \alpha'}^i \langle l', \alpha' | H | l, \alpha \rangle. \quad (\text{A2})$$

##### a. The matrix element $\langle l, \alpha | H | l', \alpha' \rangle$

*Case 1* ( $l=l'$ ): When  $l=l'$ , the matrix element is given by

$$\langle l, \alpha | H | l', \alpha' \rangle = \begin{cases} E_s & \text{if } \alpha=1, \\ E_p & \text{if } \alpha=2, 3, 4, \\ 0 & \text{if } \alpha \neq \alpha'. \end{cases} \quad (\text{A3})$$

*Case 2* ( $l \neq l'$ ): For the case  $l \neq l'$ , we assume a  $1/R^2$  dependence of the matrix element on the interatomic distance  $R$ :

$$\langle l, \alpha | H | l', \alpha' \rangle = f_c(|\mathbf{R}_{l'} - \mathbf{R}_l|) E_{l, \alpha, l', \alpha'} \frac{R_0^2}{|\mathbf{R}_{l'} - \mathbf{R}_l|^2} \quad (\text{A4})$$

where  $R_0$  is the nearest-neighbor distance in diamond-structure Si,  $R_0 = \sqrt{3}/4 \times 5.4307 \text{ \AA}$ .  $f_c$  is the cutoff function defined as

$$f_c(R) = \frac{1}{2} \left[ 1 - \tanh \left[ \frac{R - R_b}{\Delta} \right] \right]. \quad (\text{A5})$$

Let  $\{l, m, n\}$  be the direction cosines of the vector  $\mathbf{R}_{l'} - \mathbf{R}_l$ :

$$l = \frac{R_{l'x} - R_{lx}}{|\mathbf{R}_{l'} - \mathbf{R}_l|},$$

$$m = \frac{R_{l'y} - R_{ly}}{|\mathbf{R}_{l'} - \mathbf{R}_l|}, \quad (\text{A6})$$

$$n = \frac{R_{l'z} - R_{lz}}{|\mathbf{R}_{l'} - \mathbf{R}_l|}.$$

The  $E_{l, \alpha, l', \alpha'}$ 's can be determined as follows (here  $\alpha=1, 2, 3, 4$  is equivalent to  $s, x, y, z$ , respectively):

$$E_{ls, l's} = V_{ss\sigma},$$

$$E_{ls, l'x} = -E_{lx, l's} = lV_{sp\sigma},$$

$$E_{ls, l'y} = -E_{ly, l's} = mV_{sp\sigma},$$

$$E_{ls, l'z} = -E_{lz, l's} = nV_{sp\sigma},$$

$$E_{lx, l'y} = E_{ly, l'x} = lm(V_{pp\sigma} - V_{pp\pi}),$$

$$E_{lx, l'z} = E_{lz, l'x} = ln(V_{pp\sigma} - V_{pp\pi}),$$

$$E_{ly, l'z} = E_{lz, l'y} = mn(V_{pp\sigma} - V_{pp\pi}),$$

$$E_{lx, l'x} = l^2V_{pp\sigma} + (1-l^2)V_{pp\pi},$$

$$E_{ly, l'y} = m^2V_{pp\sigma} + (1-m^2)V_{pp\pi},$$

$$E_{lz, l'z} = n^2V_{pp\sigma} + (1-n^2)V_{pp\pi}. \quad (\text{A7})$$

The tight-binding parameters have the following values for Si:<sup>10</sup>

$$E_s = -5.25 \text{ eV}, \quad E_p = 1.20 \text{ eV},$$

$$V_{ss\sigma} = -1.938 \text{ eV}, \quad V_{sp\sigma} = 1.745 \text{ eV},$$

$$V_{pp\sigma} = 3.050 \text{ eV}, \quad V_{pp\pi} = -1.075 \text{ eV}. \quad (\text{A8})$$

##### 2. The repulsive term $E_2$

In this subsection we consider the second term  $E_2$ , Eq. (4), of the total energy  $E^{\text{tot}}$ ,

$$E_2 = \sum_{l=2}^N \sum_{l'=1}^{l-1} E_r(|\mathbf{R}_l - \mathbf{R}_{l'}|). \quad (\text{A9})$$

$E_2$  is the repulsive energy needed to neutralize the effect of double counting of the Coulomb interactions in the band-structure term  $E^{\text{BS}}$ . The  $E_r$  appearing in  $E_2$  is

$$E_r(R) = E_{\text{Si}_2}^{\text{tot}}(R) f_c(R) - E_{\text{Si}_2}^{\text{BS}}(R), \quad (\text{A10})$$

where  $E_{\text{Si}_2}^{\text{tot}}$  is the total energy of diatomic Si,  $E_{\text{Si}_2}^{\text{BS}}$  is the band-structure energy of diatomic Si, and  $f_c(R)$  is the cutoff function defined by (A5).

#### a. Total energy of diatomic Si

$E_{\text{Si}_2}^{\text{tot}}$  has the following expression:<sup>12</sup>

$$E_{\text{Si}_2}^{\text{tot}} = \begin{cases} A[(R/R^*)^p - (R/R^*)^q] \\ \quad \times \exp[\gamma/(a - R/R^*)^\nu] & \text{if } R/R^* < a, \\ 0 & \text{if } R/R^* \geq a, \end{cases} \quad (\text{A11})$$

with

$$\begin{aligned} A &= 80\,716.277 \text{ eV}, \\ R^* &= 1.781\,435\,4 \text{ \AA}, \\ \gamma &= -10.706\,328, \\ p &= -3.372\,065\,8, \\ q &= -0.475\,829\,60, \\ \nu &= 0.310\,406\,57, \\ a &= 2.806\,725\,4 \text{ \AA}. \end{aligned} \quad (\text{A12})$$

$E_{\text{Si}_2}^{\text{tot}}$  has a minimum value  $E_m$  of  $-3.07$  eV which occurs at  $R_0 = 2.265$  \AA and a vibrational frequency  $f$  of  $519$   $\text{cm}^{-1}$ . The vibrational frequency was found in the following manner. The curve  $E - E_m = (K/2)(R - R_0)^2$  was fitted to the function (A11) at the point  $E = E_m$  and  $R = R_0$ . Here  $K$  is the force constant. The frequency  $f$  is then given by

$$f = \frac{1}{2\pi} \left[ \frac{K}{M_r} \right]^{1/2}, \quad (\text{A13})$$

where  $M_r = M/2$  and  $M$  is the mass of a Si atom. If  $f$  has units of cycles/s, then the frequency in  $\text{cm}^{-1}$  is given by  $f/c$ , where  $c$  is the velocity of light in  $\text{cm/s}$ .

#### b. Band-structure energy of diatomic Si

Consider two Si atoms situated a distance  $R$  apart. Let one of the atoms be situated at the origin and the other at position  $R\mathbf{i} + 0\mathbf{j} + 0\mathbf{k}$ . For the basis set choose the eight-element set  $\{\phi_{l_1,1}, \phi_{l_1,2}, \phi_{l_1,3}, \phi_{l_1,4}, \phi_{l_2,1}, \phi_{l_2,2}, \phi_{l_2,3}, \phi_{l_2,4}\}$ , where  $l_1$  and  $l_2$  denote the two atoms. These basis functions have been described in Sec. II of the main text of this paper. The matrix elements  $\langle l'\alpha' | H | l\alpha \rangle$  of the  $8 \times 8$  Hamiltonian matrix are given in Sec. A1 of this Appendix. The Hamiltonian matrix splits up into the following two submatrices:

$$M_1 = \begin{pmatrix} E_s & 0 & a' & b' \\ 0 & E_p & -b' & c' \\ a' & -b' & E_s & 0 \\ b' & c' & 0 & E_p \end{pmatrix} \quad (\text{A14})$$

and

$$M_2 = \begin{pmatrix} E_p & 0 & d' & 0 \\ 0 & E_p & 0 & d' \\ d' & 0 & E_p & 0 \\ 0 & d' & 0 & E_p \end{pmatrix}, \quad (\text{A15})$$

where

$$\begin{aligned} a' &= V_{ss\sigma} f_c(R)(R_0^2/R^2), \quad b' = V_{sp\sigma} f_c(R)(R_0^2/R^2), \\ c' &= V_{pp\sigma} f_c(R)(R_0^2/R^2), \quad d' = V_{pp\pi} f_c(R)(R_0^2/R^2). \end{aligned} \quad (\text{A16})$$

The matrix  $M_1$  gives the following four energy eigenvalues,  $\lambda_1, \lambda_2, \lambda_3$ , and  $\lambda_4$ :

$$\begin{aligned} 2\lambda_1 &= (E_s + E_p) - (a' - c') \\ &\quad + \{[(E_s - E_p) - (a' + c')]^2 + 4b'^2\}^{1/2}, \\ 2\lambda_2 &= (E_s + E_p) - (a' - c') \\ &\quad - \{[(E_s - E_p) - (a' + c')]^2 + 4b'^2\}^{1/2}, \\ 2\lambda_3 &= (E_s + E_p) + (a' - c') \\ &\quad + \{[(E_s - E_p) + (a' + c')]^2 + 4b'^2\}^{1/2}, \\ 2\lambda_4 &= (E_s + E_p) + (a' - c') \\ &\quad - \{[(E_s - E_p) + (a' + c')]^2 + 4b'^2\}^{1/2}. \end{aligned} \quad (\text{A17})$$

The energy eigenvalues  $\lambda_5, \lambda_6, \lambda_7$ , and  $\lambda_8$ , of the matrix  $M_2$  are readily found to be

$$\begin{aligned} \lambda_5 &= \lambda_7 = E_p + d', \\ \lambda_6 &= \lambda_8 = E_p - d'. \end{aligned} \quad (\text{A18})$$

With the values of the tight-binding parameters given in (A8), these energy eigenvalues appear in the following order (this order was determined by plotting the eigenvalues versus  $R$  for all  $R > 2.2$  \AA):

$$\lambda_4 < \lambda_2 < \lambda_3 < \lambda_5 = \lambda_7 < \lambda_6 = \lambda_8 < \lambda_1. \quad (\text{A19})$$

Thus in the ground-state configuration the eigenvalues  $\lambda_2, \lambda_3, \lambda_4$ , and  $\lambda_5$  are occupied, each with two electrons, one with spin up and one with spin down. The band-structure energy of the diatomic molecule at interatomic separation  $R$  is therefore given by

$$\begin{aligned} E_{\text{Si}_2}^{\text{BS}} + 2E_{\text{Si}}^0 &= 2(\lambda_2 + \lambda_3 + \lambda_4 + \lambda_5) \\ &= a' + 2d' - c' + 3E_s + 5E_p \end{aligned} \quad (\text{A20})$$

$$- \{[(E_s - E_p) - (a' + c')]^2 + 4b'^2\}^{1/2}. \quad (\text{A21})$$

*Note:* A second way to determine  $E_{\text{Si}_2}^{\text{BS}}$  is to invoke the variational principle, i.e., vary the coefficients  $\{c_{l\alpha}^i\}$  in (1) until the minimum of the band-structure energy is achieved. This method gives the "occupied eigenvalues"  $\{\lambda_i'\}$ ,

$$\lambda_i' = \sum_{l', \alpha'} \sum_{l, \alpha} c_{l\alpha}^i c_{l'\alpha'}^i \langle l'\alpha' | H | l\alpha \rangle, \quad i = 1, 2, 3, 4 \quad (\text{A22})$$

and the band-structure energy

$$E_{\text{Si}_2}^{\text{BS}} + 2E_{\text{Si}}^0 = 2(\lambda'_1 + \lambda'_2 + \lambda'_3 + \lambda'_4). \quad (\text{A23})$$

Here, the coefficients  $\{c_{i\alpha}^i\}$  have the values which give the minimum band-structure energy.

The two equations (A20) and (A23) should give identical results for the band-structure energy  $E_{\text{Si}_2}^{\text{BS}}$ ; however, the occupied eigenvalues  $\{\lambda'_i\}$  obtained via (A22) may not be equal to the actual eigenvalues  $\{\lambda_i\}$ , (A17) and (A18), of the Hamiltonian. This is illustrated in the following exercise. The band-structure energy (A1) of the diatomic Si molecule was minimized at an interatomic separation of 2.265 Å to get the "occupied eigenvalues" having the values

$$\begin{aligned} \lambda'_1 &= -1.115 \text{ eV}, & \lambda'_2 &= -1.115 \text{ eV}, \\ \lambda'_3 &= -5.375 \text{ eV}, & \lambda'_4 &= -5.375 \text{ eV}. \end{aligned} \quad (\text{A24})$$

The actual eigenvalues, (A17) and (A18), of the Hamiltonian were also calculated at the same interatomic separation to give

$$\begin{aligned} \lambda_5 &= 0.04 \text{ eV}, & \lambda_3 &= -1.48 \text{ eV}, \\ \lambda_2 &= -3.60 \text{ eV}, & \lambda_4 &= -7.94 \text{ eV}. \end{aligned} \quad (\text{A25})$$

Notice that the 'occupied eigenvalues' (A24) are different from the actual occupied eigenvalues (A25), although use of (A20) and (A23) shows that both sets of eigenvalues give the same band-structure energy  $E_{\text{Si}_2}^{\text{BS}} + 2E_{\text{Si}}^0$  of  $-25.96 \text{ eV}$ .

### 3. The terms $E_3$ and $E_4$

The third term (5) of the total energy (2) is

$$E_3 = N \left[ \phi_1 \left[ \frac{n_b}{N} \right]^2 + \phi_2 \left[ \frac{n_b}{N} \right] + \phi_3 \right]. \quad (\text{A26})$$

Here,  $n_b$  is the number of bonds,

$$n_b = \sum_{l=2}^N \sum_{l'=1}^{l-1} f_c(|\mathbf{R}_l - \mathbf{R}_{l'}|). \quad (\text{A27})$$

The cutoff function  $f_c$  has been defined by Eq. (A5). The other parameters in (A26) have the following values:<sup>2</sup>

$$\begin{aligned} \phi_1 &= 0.225 \text{ eV}, \\ \phi_2 &= 1.945 \text{ eV}, \\ \phi_3 &= -1.03 \text{ eV}. \end{aligned} \quad (\text{A28})$$

Note that with the above choice of parameters the term  $E_3$  goes to zero for  $\text{Si}_2$  ( $N=2$  and  $n_b=1$ ).

The fourth term (6) of the total energy (2) has already been defined via Eqs. (6) and (10). These equations are repeated here for completeness:

$$E_4 = U \sum_{i=1}^N (q_i - q_i^0)^2, \quad (\text{A29})$$

where

$$q_i = 2 \sum_{\alpha=1}^{2N} \sum_{\alpha=1}^4 (c_{i\alpha}^i)^2, \quad q_i^0 = 4.0. \quad (\text{A30})$$

Note that this term is equal to zero for uncharged clusters and has a positive value for charged clusters; thus this term prevents charge transfer among the atoms.

\*Present address: Sacks/Freeman Associates, Landover, MA 20785.

<sup>1</sup>R. Biswas and D. R. Hamann, Phys. Rev. Lett. **55**, 2001 (1985).

<sup>2</sup>S. L. Altmann, A. Lapicciarella, K. W. Lodge, and N. Tomasini, J. Phys. C **15**, 5581 (1982).

<sup>3</sup>F. H. Stillinger and T. A. Weber, Phys. Rev. B **31**, 5262 (1985).

<sup>4</sup>X. P. Li, G. Chen, P. B. Allen, and J. Q. Broughton, Phys. Rev. B **38**, 3331 (1988).

<sup>5</sup>R. O. Jones, Phys. Rev. A **32**, 2589 (1985).

<sup>6</sup>K. Raghavachari, J. Chem. Phys. **83**, 3520 (1985).

<sup>7</sup>R. Car and M. Parrinello, Phys. Rev. Lett. **55**, 2471 (1985); **60**, 204 (1988).

<sup>8</sup>D. Tománek and M. A. Schlüter, Phys. Rev. Lett. **56**, 1055 (1986); D. Tománek and M. A. Schlüter, Phys. Rev. B **36**, 1208 (1987).

<sup>9</sup>O. L. Alerhand and E. J. Mele, Phys. Rev. B **35**, 1 (1986).

<sup>10</sup>D. J. Chadi, Phys. Rev. B **29**, 785 (1984).

<sup>11</sup>D. J. Chadi, Phys. Rev. Lett. **43**, 43 (1979).

<sup>12</sup>Reference 8 credits this dimer total energy to K. Raghavachari (private communication).

chari (private communication).

<sup>13</sup>D. C. Allan and E. J. Mele, Phys. Rev. B **31**, 5565 (1985).

<sup>14</sup>C. G. Broyden, Math. Comput. **19**, 577 (1965).

<sup>15</sup>D. Beeman, J. Comput. Phys. **20**, 130 (1976).

<sup>16</sup>L. Verlet, Phys. Rev. **159**, 98 (1967).

<sup>17</sup>J.-P. Ryckaert, G. Ciccotti, and H. J. C. Berendsen, J. Comput. Phys. **23**, 327 (1977).

<sup>18</sup>P. O. Löwdin, J. Chem. Phys. **18**, 365 (1950); Adv. Quantum Chem. **5**, 185 (1970).

<sup>19</sup>M. C. Payne, J. D. Joannopoulos, D. C. Allan, M. P. Teter, and D. H. Vanderbilt, Phys. Rev. Lett. **56**, 2656 (1986).

<sup>20</sup>F. F. Abraham, Adv. Phys. **35**, 1 (1986).

<sup>21</sup>M. T. Yin and M. L. Cohen, Phys. Rev. B **24**, 2303 (1981).

<sup>22</sup>R. M. Tromp, R. J. Hamers, and J. E. Demuth, Phys. Rev. Lett. **55**, 1303 (1985).

<sup>23</sup>J. Ihm, D. H. Lee, J. D. Joannopoulos, and J. J. Xiong, Phys. Rev. Lett. **51**, 1872 (1983).

<sup>24</sup>I. Stich, Magister Philosophiae thesis, ISAS-International School for Advanced Studies, 1986/87.